CrystEngComm

PAPER

View Article Online
View Journal | View Issue

Cite this: *CrystEngComm*, 2014, **16**, 9104

Investigation of the structure variation of metal diphosphonates with the changing of N-donor auxiliary ligands and their properties†

Si-Fu Tang,*[a] Liang-Jun Li,[b] Chao Wang[a] and Xue-Bo Zhao*[b]

Received 20th June 2014,
Accepted 5th August 2014

DOI: 10.1039/c4ce01266f

www.rsc.org/crystengcomm

Nine metal diphosphonates, $[Co(H_2L)(pyz)(H_2O)][(H_2O)_{0.5}]$ (**1**), $[Ni(H_2L)(pyz)(H_2O)_2]$ (**2**), $[Ni(H_2L)(2,2'\text{-bipy})_2][(H_2O)_2]$ (**3**), $[Ni(H_2L)(4,4'\text{-bipy})(H_2O)][(H_2O)_2]$ (**4**), $[Ni(H_2L)(dpe)(H_2O)_2][(H_2O)_2]$ (**5**), $[Cu(H_2L)(pyz)(H_2O)_2]$ (**6**), $[Cu(H_2L)(4,4'\text{-bipy})][(H_2O)_2]$ (**7**), $[Zn(H_2L)(2,2'\text{-bipy})(H_2O)_2]$ (**8**) and $[Cd(H_2L)(pyz)(H_2O)_2]$ (**9**), have been synthesized from a diphosphonate ligand 2,5-dimethyl-1,4-phenylenediphosphonic acid (H_4L) and four N-donor auxiliary ligands (pyz = pyrazine, 2,2′-bipy = 2,2′-bipyridine, 4,4′-bipy = 4,4′-bipyridine, dpe = 1,2-di(4-pyridyl)ethylene). In compound **1**, pyrazine molecules behave as pillars which connect the $Co(H_2L)$ layers into a 3D network structure. Compounds **2**, **6** and **9** are isostructural and also show 3D framework structures, in which metal centers are linked by the bidentate diphosphonate ligands into 1D infinite chains and are connected by the pyrazine linkers. In compounds **3** and **8**, the diphosphonate ligands, showing bidentate or tetradentate coordination modes, bridge the respective metal ions (Ni^{2+} and Zn^{2+}) into a 1D infinite chain or 2D layer structure, respectively, in which the 2,2′-bipy ligands chelate to the central metal ions and complete the coordination spheres. In compound **4**, the 4,4′-bipy molecules also behave as pillars between the 2D layers, which are constructed from tridentate bridging diphosphonate ligands and six-coordinated Ni^{2+} ions. Compounds **5** and **7** have similar square grid layered structures which are constructed from bridging bidentate diphosphonate ligands and 4,4′-bipy or dpe linkers. Photophysical measurements indicate that compounds **8** and **9** display ligand centered emissions. Magnetic studies reveal that dominant antiferromagnetic interactions are propagated in compounds **1**–**3** between the magnetic centers.

Introduction

Metal phosphonates, as one kind of important inorganic–organic hybrid materials, have received tremendous attention[1] due to not only their fascinating structures, but also their promising applications as functional materials in a wide range of fields, including gas separation/sorption,[2] catalysis,[3] optical applications,[4] magnetism[5] and so on, which are all structure sensitive. Many metal phosphonates have been constructed by decorating the phosphonate ligand with other coordinating functional groups[6] or introducing a second auxiliary ligand.[7] In principle, a near limitless number of metal phosphonates can be obtained through different combinations of metal ions and organic ligands. Therefore, it is important to understand the mechanism of structure assembly and the structure–property relationships of this class of material for the final purpose of designing and synthesizing materials according to requirement. Comparing with the carboxylic acid group, the phosphonic acid group has an additional oxygen atom, giving it one more coordinating site and consequently more coordination modes, which makes it a great challenge to design and synthesize materials with specific structure and function. Many factors, such as the coordination geometry of the central metal ions, connective modes of the organic ligands, and synthesis conditions, can affect the final structures. Many efforts have been made to understand these by investigating different metal centers, functionalized phosphonate ligands, and synthesis conditions. The auxiliary ligand also has a large effect on the final structure, but until now systematic investigation of the effects of auxiliary ligands on the structure formation is still under explored.

Very recently we reported eight metal diphosphonates synthesized from 2,5-dimethyl-1,4-phenylenediphosphonic acid (H_4L).[8] Among the eight compounds, the diphosphonate ligand mainly adopted tetradentate (μ^4:η^0:η^1:η^1:η^0:η^1:η^1) or bidentate

[a] *Key Laboratory of Biofuel, Chinese Academy of Sciences, Qingdao Institute of Bioenergy and Bioprocess Technology, 266101, Qingdao, China.*
E-mail: tangsf@qibebt.ac.cn; Fax: +86 0532 80662728; Tel: +86 0532 80662728
[b] *Institute of Unconventional Hydrocarbon and New Energy Sources, China University of Petroleum (East China), Qingdao 266580, China.*
E-mail: zhaoxuebo@upc.edu.cn

† Electronic supplementary information (ESI) available: O–H···O bonds, PXRD and X-ray crystallographic files for **1**–**9** in CIF format. CCDC 1005981–1005989. For ESI and crystallographic data in CIF or other electronic format see DOI: 10.1039/c4ce01266f

(μ^2:η^0:η^0:η^1:η^0:η^0:η^1) coordination modes, providing a good platform to investigate the effect of auxiliary ligands on the structure formation. Therefore, we reacted it with some transition metal salts and N-donor auxiliary ligands of different sizes, including pyrazine, 2,2′-bipyridine, 4,4′-bipyridine and 1,2-di(4-pyridyl)ethylene. Luckily, one series of new metal diphosphonates, namely $[Co(H_2L)(pyz)(H_2O)][(H_2O)_{0.3}]$ (**1**), $[Ni(H_2L)(pyz)(H_2O)_2]$ (**2**), $[Ni(H_2L)(2,2'\text{-bipy})_2][(H_2O)_2]$ (**3**), $[Ni(H_2L)(4,4'\text{-bipy})(H_2O)][(H_2O)_2]$ (**4**), $[Ni(H_2L)(dpe)(H_2O)_2][(H_2O)_2]$ (**5**), $[Cu(H_2L)(pyz)(H_2O)_2]$ (**6**), $[Cu(H_2L)(4,4'\text{-bipy})][(H_2O)_2]$ (**7**), $[Zn(H_2L)(2,2'\text{-bipy})(H_2O)_2]$ (**8**) and $[Cd(H_2L)(pyz)(H_2O)_2]$ (**9**), were obtained successfully. Herein, we report on their syntheses and structures, luminescent and magnetic properties.

Experimental

Materials and instruments

The synthesis of 2,5-dimethyl-1,4-phenylenediphosphonic acid (H_4L) has been reported elsewhere.[8] Elemental analyses were performed on a Vario EL III elemental analyzer. IR spectra were recorded on a Nicolet 6700 FTIR spectrometer as KBr pellets in the range of 4000–400 cm^{-1}. Powder X-ray patterns were obtained on a Bruker D8 Advance diffractometer using Cu-Kα radiation. Solution ^1H NMR spectra were recorded on a Bruker AVANCE-III NMR (600 MHz). Thermogravimetric analyses (TGA) were carried out on a NETZSCH STA 449C unit at a heating rate of 10 °C min^{-1} under a nitrogen atmosphere. Fluorescent analyses of the free diphosponate ligand (H_4L), pyrazine, 2,2′-bipy and compounds **8** and **9** were performed on Fluoromax-4 spectrofluorometer. Variable temperature magnetic susceptibility measurements of compounds **1–3** were obtained in the solid state using a Quantum Design SQUID MPMS-7 magnetometer operating at 1000 Oe.

Single-crystal structure determination

Single crystal X-ray diffraction measurements of compounds **1–9** were carried out on a Bruker SMART APEX II CCD diffractometer (Mo-Kα radiation, λ = 0.0713 Å) at room temperature. SAINT was used for the integration of intensity of reflections and scaling.[9] Absorption corrections were carried out with the program SADABS.[10] Crystal structures were solved by direct methods using SHELXS.[11] Subsequent difference Fourier analyses and least squares refinement with SHELXL-97 (ref. 12) allowed for the location of the atom positions. In the final step of the crystal structure refinement hydrogen atoms of idealized $-CH_2$ and $-CH_3$ groups were added and treated with the riding atom mode; their isotropic displacement factors were chosen as 1.2 and 1.5 times the preceding carbon atom, respectively. All non-hydrogen atoms were refined with anisotropic thermal parameters. The hydrogen atoms on the water molecules of **1–9**, except O2w in **1**, were located from the difference Fourier map and not included in the refinements. One lattice water molecule (O2w) in compound **1** is partially occupied; its site-occupation factor is refined to be 0.3. The crystallographic details for compounds **1–9** are summarized in Table 1. The data have been deposited into the Cambridge Crystallographic Data Centre (CCDC) with deposition numbers CCDC 1005981–1005989 for compounds **1–9**.†

Synthesis of compound $[Co(H_2L)(pyz)(H_2O)][(H_2O)_{0.3}]$ (1). H_4L (0.0665 g, 0.25 mmol), $CoCl_2{\cdot}6H_2O$ (0.0595 g, 0.25 mmol), pyrazine (0.0200 g, 0.25 mmol) and 6 mL of water were mixed and stirred in a Teflon-lined autoclave. Afterwards, it was sealed and heated at 160 °C for 3 days and allowed to cool to room temperature in a time period of 24 hours. The initial and final pH values of the resultant solutions were about 4.0 and 3.0, respectively. Pink block crystals (0.044 g) were collected in satisfying yield (41%, based on metal source) and washed with deionized water. Elemental analysis (%) calcd for $C_{12}H_{16.6}CoN_2O_{7.3}P_2$ (426.54): C 33.79, H 3.92, N 6.57%; found: C 33.71, H 4.09, N 6.62%. IR (KBr, cm^{-1}): 3580.4 (m), 3432.3 (b, m), 3101.9 (m), 2924.9 (m), 2290.2 (b, w), 1640.1 (m), 1482.9 (w), 1447.1 (m), 1411.4 (m), 1386.1 (w), 1359.5 (w), 1262.1 (w), 1220.8 (m), 1177.1 (s), 1151.0 (m), 1129.5 (m), 1120.8 (m), 1093.7 (m), 1076.2 (m), 1047.1 (sh, s), 1038.4 (s), 1011.5 (m), 928.4 (m), 906.1 (w), 883.1 (s), 808.4 (m), 771.4 (w), 734.0 (w), 675.4 (vw), 602.4 (s), 518.6 (w), 498.9 (w), 463.5 (m).

Synthesis of compound $[Ni(H_2L)(pyz)(H_2O)_2]$ (2). The synthesis of compound **2** is similar to that of **1** except the displacement of $CoCl_2{\cdot}6H_2O$ with $NiSO_4{\cdot}6H_2O$. The initial and final pH values of the resultant solutions were about 4.0 and 3.0, respectively. Green block crystals (0.049 g) were collected in satisfying yield (45%, based on metal source) and washed with deionized water. Elemental analysis (%) calcd for $C_{12}H_{18}N_2NiO_8P_2$ (438.93): C 32.84, H 4.13, N 6.38%; found: C 32.91, H 4.19, N 6.44%. IR (KBr, cm^{-1}): 3468.1 (s), 3133.2 (m), 3070.0 (m), 2924.4 (m), 2862.2 (b, m), 2393.0 (m), 2317.0 (m), 1830.8 (w), 1648.4 (w), 1492.5 (w), 1449.4 (vw), 1419.0 (w), 1386.4 (w), 1356.8 (w), 1218.9 (m), 1204.6 (sh, m), 1153.1 (s), 1132.2 (sh, s), 1095.6 (m), 1061.1 (m), 1004.0 (s), 913.5 (s), 860.7 (m), 816.4 (m), 773.3 (w), 705.3 (w), 680.2 (w), 625.0 (m), 580.4 (m), 506.4 (m), 475.2 (m), 434.3 (m).

Synthesis of compound $[Ni(H_2L)(2,2'\text{-bipy})_2][(H_2O)_2]$ (3). The synthesis of compound **3** is similar to that of **2** except the displacement of pyrazine with 2,2′-bipy. The initial and final pH values of the resultant solutions were about 4.0 and 3.0, respectively. Green block crystals (0.074 g) were collected in satisfying yield (88%, based on 2,2′-bipy) and washed with deionized water. Elemental analysis (%) calcd for $C_{28}H_{30}N_4NiO_8P_2$ (671.21): C 50.11, H 4.51, N 8.35%; found: C 50.19, H 4.60, N 8.37%. IR (KBr, cm^{-1}): 3424.8 (b, s), 3116.0 (m), 3071.9 (m), 3037.2 (m), 2923.1 (m), 2388.2 (w), 1636.3 (w), 1600.9 (m), 1576.8 (vw), 1566.8 (vw), 1493.8 (vw), 1475.0 (w), 1442.7 (s), 1380.9 (w), 1352.9 (w), 1316.5 (w), 1249.9 (w), 1153.5 (s), 1126.8 (m), 1070.5 (m), 1023.2 (s), 966.6 (w), 881.5 (m), 766.7 (m), 736.4 (m), 654.0 (w), 623.5 (w), 591.8 (s), 494.5 (w).

Synthesis of compound $[Ni(H_2L)(4,4'\text{-bipy})(H_2O)][(H_2O)_2]$ (4). The synthesis of compound **4** is similar to that of **2** except the displacement of pyrazine with 4,4′-bipy. The initial and final pH values of the resultant solutions were about 4.0 and 3.0, respectively. Green block crystals (0.111 g) were

Table 1 Crystallographic parameters of compounds 1–9[a,b]

Compound	1	2	3	4	5
Formula	$C_{12}H_{16.6}CoN_2O_{7.3}P_2$	$C_{12}H_{18}N_2NiO_8P_2$	$C_{28}H_{30}N_4NiO_8P_2$	$C_{18}H_{24}N_2NiO_9P_2$	$C_{20}H_{28}N_2NiO_{10}P_2$
Fw	426.54	438.93	671.21	533.04	577.09
Space group	$P2_1/c$	$C2/c$	$R3c$	$P\bar{1}$	$P\bar{1}$
a (Å)	11.7903(15)	17.119(2)	23.7747(14)	10.3111(16)	10.3161(14)
b (Å)	9.3140(13)	8.9053(12)	23.7747(14)	10.7447(17)	11.508(3)
c (Å)	14.652(2)	12.3890(17)	28.216(4)	11.805(2)	12.0717(16)
α (deg)	90	90	90	71.192(4)	105.480(3)
β (deg)	94.385(2)	124.674(2)	90	65.659(4)	109.935(2)
γ (deg)	90	90	120	83.226(4)	101.391(4)
V (Å^3)	1604.3(4)	1553.3(4)	13 812(2)	1127.8(3)	1230.8(4)
Z	4	4	18	2	2
D_{calcd}, (g cm^{-3})	1.766	1.877	1.453	1.570	1.557
Abs coeff (mm^{-1})	1.310	1.504	0.791	1.054	0.979
Reflns collected	8209	7067	20 167	9016	9768
Independent reflns/R_{int}	2737/0.0578	1766/0.0478	5033/0.1277	3956/0.0836	4325/0.0573
GOF on F^2	1.040	1.064	1.013	0.973	0.980
R_1, wR_2 [$I > 2\sigma(I)$]	0.0390, 0.0941	0.0319, 0.0831	0.0666, 0.1512	0.0586, 0.1150	0.0492, 0.1002
R_1, wR_2 (all data)	0.0508, 0.1018	0.0353, 0.0851	0.1272, 0.1891	0.1078, 0.1341	0.0879, 0.1115

Compound	6	7	8	9
Formula	$C_{12}H_{18}N_2CuO_8P_2$	$C_{18}H_{22}CuN_2O_8P_2$	$C_{18}H_{18}N_2O_6P_2Zn$	$C_{12}H_{18}N_2CdO_8P_2$
Fw	443.76	519.85	485.65	492.62
Space group	$C2/c$	$P\bar{1}$	$P\bar{1}$	$C2/c$
a (Å)	16.906(11)	7.309(3)	9.1979(7)	17.447(2)
b (Å)	8.996(6)	8.365(4)	10.0023(9)	8.7795(11)
c (Å)	12.435(8)	9.315(4)	12.2994(9)	12.845(3)
α (deg)	90	97.459(6)	85.738(3)	90
β (deg)	125.406(12)	112.125(6)	77.906(2)	123.7030(10)
γ (deg)	90	90.768(7)	65.089(3)	90
V (Å^3)	1541.5(17)	521.9(4)	1003.37(14)	1636.9(5)
Z	4	1	2	4
D_{calcd}, (g cm^{-3})	1.912	1.654	1.607	1.999
Abs coeff (mm^{-1})	1.673	1.249	1.422	1.576
Reflns collected	3910	3922	8276	7450
Independent reflns/R_{int}	1351/0.0586	1817/0.0518	3458/0.0513	1870/0.0490
GOF on F^2	1.056	1.064	1.020	1.039
R_1, wR_2 [$I > 2\sigma(I)$]	0.0442, 0.1019	0.0519, 0.1276	0.0416, 0.0817	0.0296, 0.0724
R_1, wR_2 (all data)	0.0628, 0.1104	0.0745, 0.1352	0.0752, 0.0891	0.0368, 0.0761

[a] $R_1 = \sum||F_o| - |F_c||/\sum|F_o|$. [b] $wR_2 = \{\sum[w(F_o^2 - F_c^2)^2]/\sum w(F_o^2)^2\}1/2$.

collected in satisfying yield (83%, based on metal source) and washed with deionized water. Elemental analysis (%) calcd for $C_{18}H_{24}N_2NiO_9P_2$ (533.04): C 40.56, H 4.54, N 5.26%; found: C 40.59, H 4.66, N 5.33%. IR (KBr, cm^{-1}): 3667.3 (w), 3473.9 (s), 2962.4 (w), 2923.8 (m), 2858.0 (w), 2386.3 (b, w), 1646.4 (w), 1607.0 (s), 1537.6 (w), 1484.6 (w), 1456.7 (w), 1413.2 (w), 1379.2 (vw), 1347.0 (w), 1217.5 (m), 1158.1 (vs), 1136.6 (sh, s), 1093.5 (m), 1071.6 (m), 1047.0 (s), 973.2 (w), 918.8 (s), 890.0 (m), 853.0 (w), 817.7 (m), 742.2 (w), 660.7 (vw), 634.6 (m), 622.7 (w), 598.0 (s), 573.4 (m), 537.6 (m), 485.5 (m).

Synthesis of compound $[Ni(H_2L)(dpe)(H_2O)_2][(H_2O)_2]$ (5). The synthesis of compound 5 is similar to that of 2 except the displacement of pyrazine with dpe. The initial and final pH values of the resultant solutions were about 4.0 and 3.0, respectively. Green block crystals (0.075 g) were collected in satisfying yield (52%, based on metal source) and washed with deionized water. Elemental analysis (%) calcd for $C_{18}H_{24}N_2NiO_9P_2$ (577.09): C 41.63, H 4.89, N 4.85%; found: C 41.70, H 4.99, N 4.82%. IR (KBr, cm^{-1}): 3423.5 (b, m), 3083.6 (w), 2387.1 (b, m), 1611.9 (vs), 1506.5 (vw), 1475.4 (vw), 1457.5 (vw), 1427.1 (w), 1382.5 (vw), 1352.7 (w), 1246.7 (m), 1206.9 (w), 1158.5 (s), 1135.0 (vs), 1077.0 (s), 1019.6 (m), 988.2 (m), 901.4 (m), 830.8 (m), 669.0 (w), 624.9 (m), 585.9 (s), 554.4 (w), 525.6 (m), 498.5 (w), 440.2 (vw).

Synthesis of compound $[Cu(H_2L)(pyz)(H_2O)_2]$ (6). The synthesis of compound 6 is similar to that of 1 except the displacement of $CoCl_2{\cdot}6H_2O$ with $CuSO_4{\cdot}6H_2O$. The initial and final pH values of the resultant solutions were about 4.0 and 3.0, respectively. Blue block crystals (0.063 g) were collected in satisfying yield (57%, based on metal source) and washed with deionized water. Elemental analysis (%) calcd for $C_{12}H_{18}N_2CuO_8P_2$ (443.76): C 32.48, H 4.09, N 6.31%; found: C 32.57, H 4.16, N 6.32%. IR (KBr, cm^{-1}): 3481.5 (s), 3182.4 (m), 3117.0 (m), 3052.6 (m), 1648.3 (w), 1491.4 (w), 1421.5 (w), 1387.7 (w), 1357.5 (w), 1261.0 (vw), 1165.4 (s), 1147.0 (s, sh), 1087.7 (m), 1060.8 (m), 1007.4 (s), 913.5 (s), 826.2 (w), 757.4 (w), 624.2 (w), 587.6 (m), 499.7 (m), 469.9 (m), 432.0 (vw).

Synthesis of compound [Cu(H$_2$L)(4,4′-bipy)][(H$_2$O)$_2$] (7). The synthesis of compound 7 is similar to that of 4 except the displacement of $NiSO_4 \cdot 6H_2O$ with $CuSO_4 \cdot 5H_2O$. The initial and final pH values of the resultant solutions were about 4.0 and 3.0, respectively. Blue block crystals (0.081 g) were collected in satisfying yield (62%, based on metal source) and washed with deionized water. Elemental analysis (%) calcd for $C_{18}H_{22}CuN_2O_8P_2$ (519.85): C 41.59, H 4.27, N 5.39%; found: C 41.51, H 4.40, N 5.46%. IR (KBr, cm^{-1}): 3630.2 (m), 3384.9 (m), 2932.7 (w), 2386.5 (w), 1613.4 (s), 1540.7 (w), 1494.0 (vw), 1479.7 (vw), 1458.2 (m), 1420.8 (m), 1381.4 (w), 1353.9 (w), 1261.4 (w), 1232.3 (vw), 1221.6 (w), 1194.7 (vw), 1120.3 (s), 1073.9 (vs), 918.7 (s), 892.9 (m), 818.1 (m), 730.3 (w), 668.6 (vw), 648.8 (w), 633.1 (w), 591.5 (s), 491.8 (m), 437.0 (m).

Synthesis of compound [Zn(H$_2$L)(2,2′-bipy)(H$_2$O)$_2$] (8). The synthesis of compound 8 is similar to that of 3 instead of the replacement of $NiSO_4 \cdot 6H_2O$ with $ZnCl_2$. The initial and final pH values of the resultant solutions were about 4.0 and 3.0, respectively. Colorless block crystals (0.046 g) were collected in satisfying yield (38%, based on metal source) and washed with deionized water. Elemental analysis (%) calcd for $C_{18}H_{18}N_2O_6P_2Zn$ (485.65): C 44.51, H 3.74, N 5.77; found: C 44.56, H 3.88, N 5.71. IR (KBr, cm^{-1}): 3073.5 (w), 2928.8 (w), 2299.2 (vw), 1606.6 (m), 1598.1 (m), 1578.1 (m), 1568.2 (w), 1491.8 (vw), 1472.7 (m), 1446.3 (m), 1377.2 (vw), 1354.3 (w), 1315.6 (w), 1280.7 (w), 1243.6 (m), 1189.9 (m, sh), 1164.9 (s), 1132.6 (s), 1074.3 (m, sh), 1046.8 (s), 1022.7 (m, sh), 933.9 (m), 903.5 (s), 760.7 (m), 734.5 (w), 653.1 (w), 628.0 (w), 598.9 (m, sh), 584.7 (s), 497.4 (w).

Synthesis of compound [Cd(H$_2$L)(pyz)(H$_2$O)$_2$] (9). The synthesis of compound 9 is similar to that of 1 except the displacement of $CoCl_2 \cdot 6H_2O$ with $CdCl_2 \cdot 0.5H_2O$. The initial and final pH values of the resultant solutions were about 4.0 and 3.0, respectively. Colorless block crystals (0.057 g) were collected in satisfying yield (46%, based on metal source) and washed with deionized water. Elemental analysis (%) calcd for $C_{12}H_{18}N_2CdO_8P_2$ (492.62): C 29.26, H 3.68, N 5.69%; found: C 29.34, H 3.71, N 5.63%. IR (KBr, cm^{-1}): 3483.2 (s), 3057.1 (m), 2288.7 (b, m), 1636.4 (m), 1482.1 (vw), 1430.5 (m), 1388.1 (w), 1352.9 (w), 1195.6 (m), 1135.9 (vs), 1090.7 (m), 1057.6 (m), 996.0 (s), 923.6 (s), 860.0 (m), 811.4 (m), 759.2 (w), 700.0 (vw), 668.7 (vw), 627.6 (m), 581.6 (s), 504.3 (m), 473.6 (s), 447.3 (m), 433.0 (m).

Results and discussion

Structural description of compound 1

Compound 1 crystallizes in the monoclinic $P2(1)/c$ space group with four molecules in each unit cell. In the asymmetric unit, one crystallographically unique Co^{2+} ion, two moieties of deprotonated diphosphonate ligand lying on inversion centers, one pyrazine, one coordinating aqua ligand and one lattice water molecule with 0.3 occupancy are present (see Fig. 1). Each Co^{2+} ion is six-coordinated by three phosphonate oxygen atoms from three diphosphonate ligands, two nitrogen atoms of two pyrazine molecules and one coordinating water molecule. The Co–O and Co–N distances are found in the ranges of 2.012(2)–2.177(2) and 2.247(3)–2.291(3) Å (see Table 2), respectively, which are all comparable to those of other reported cobalt(II) phosphonates.[13] The phosphonic acid group in each diphosphonate segment is singly deprotonated, but displays two kinds of coordination modes: tetradentate (see model-A in Scheme 1) and bidentate (see model-B in Scheme 1). The tetradentate diphosphonate ligands bridge the Co^{2+} ions into a two-dimensional layer in the *bc*-plane (see Fig. 2a), whereas the bidentate ligands further assemble these layers into a three-dimensional framework structure (see Fig. 2b). The pyrazine molecules behave as pillars between the CoO_4N_2 octahedrons in the two-dimensional layer, reinforcing the robustness of the framework.

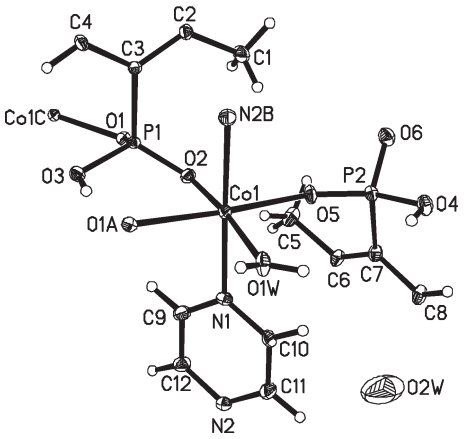

Fig. 1 XPREP diagram of 1 (thermal ellipsoids are given at 30% probability). A: 1 − *x*, 0.5 + *y*, 0.5 − *z*; B: *x*, 0.5 − *y*, −0.5 + *z*; C: 1 − *x*, −0.5 + *y*, 0.5 − *z*.

Structure description of compounds 2, 6 and 9

Compounds 2, 6 and 9 are isostructural, therefore only the structure of 2 will be described in detail. Compound 2 crystallizes in the monoclinic space group $C2/c$ with four molecules in each unit cell. There is one crystallographically independent Ni(II) ion lying in a special position (0.25, 0.25, 0), part of a diphosphonate ligand and pyrazine on their respective inversion centers and one coordinating water molecule (see Fig. 3), corresponding to a formula of [Ni(H$_2$L)(pyrazine)(H$_2$O)$_2$]. The Ni(II) ion is octahedrally coordinated by two phosphonate oxygen atoms from two diphosphonate ligands, two nitrogen atoms of two pyrazine molecules and two aqua ligands. It is found that the Ni–O (H_2L^{2-}), Ni–O (water) and Ni–N bond lengths are 2.0845(15), 2.0892(16) and 2.1701(19) Å (see Table 2), respectively, which are all in normal ranges.[14] The coordination mode of the diphosphonate ligand is the same as that found in compound 1, which can be denoted as: μ^2:η^0:η^0:η^1:η^0:η^0:η^1 (see model-B in Scheme 1). These bridging diphosphonate ligands link the Ni(II) ions into one-dimensional chains extending across two directions (see Fig. 4a and S1†). These 1D chains are further bound

Table 2 Selected bond lengths of compounds **1**–**9**[a]

1			
Co(1)–O(5)	2.012(2)	Co(1)–O(1)#1	2.177(2)
Co(1)–O(2)	2.052(2)	Co(1)–N(1)	2.247(3)
Co(1)–O(1W)	2.080(2)	Co(1)–N(2)#2	2.291(3)
2			
Ni(1)–O(1)	2.0845(15)	Ni(1)–O(1W)#1	2.0890(16)
Ni(1)–O(1)#1	2.0845(15)	Ni(1)–N(1)#1	2.1706(19)
Ni(1)–O(1W)	2.0890(16)	Ni(1)–N(1)	2.1706(19)
3			
Ni(1)–N(3)	2.059(8)	Ni(1)–N(4)	2.095(8)
Ni(1)–O(2)	2.069(6)	Ni(1)–N(1)	2.109(9)
Ni(1)–N(2)	2.083(8)	Ni(1)–O(6)#1	2.119(6)
4			
Ni(1)–O(3)#1	2.065(3)	Ni(2)–O(4)#4	2.034(3)
Ni(1)–O(3)	2.065(3)	Ni(2)–O(4)	2.034(3)
Ni(1)–O(6)#2	2.083(3)	Ni(2)–O(1W)	2.041(3)
Ni(1)–O(6)#3	2.083(3)	Ni(2)–O(1W)#4	2.041(3)
Ni(1)–N(1)	2.107(4)	Ni(2)–N(2)#5	2.114(4)
Ni(1)–N(1)#1	2.107(4)	Ni(2)–N(2)#6	2.114(4)
5			
Ni(1)–O(6)	2.048(3)	Ni(1)–O(2W)	2.109(3)
Ni(1)–O(3)	2.072(3)	Ni(1)–N(1)	2.108(3)
Ni(1)–O(1W)	2.097(3)	Ni(1)–N(2)	2.118(3)
6			
Cu(1)–O(1)	1.981(3)	Cu(1)–N(1)#1	2.113(4)
Cu(1)–O(1)#1	1.981(3)	Cu(1)–O(1W)	2.427(4)
Cu(1)–N(1)	2.113(4)	Cu(1)–O(1W)#1	2.427(4)
7			
Cu(1)–O(3)#1	1.935(3)	Cu(1)–N(1)#1	1.998(3)
Cu(1)–O(3)	1.935(3)	Cu(1)–N(1)	1.998(3)
8			
Zn(1)–O(1)#1	1.955(2)	Zn(1)–N(2)	2.117(3)
Zn(1)–O(6)	1.999(2)	Zn(1)–N(1)	2.174(3)
Zn(1)–O(3)	2.038(2)		
9			
Cd(1)–O(1)	2.282(2)	Cd(1)–N(1)#1	2.332(3)
Cd(1)–O(1)#1	2.282(2)	Cd(1)–O(1W)	2.348(2)
Cd(1)–N(1)	2.332(3)	Cd(1)–O(1W)#1	2.348(2)

[a] Symmetry transformations used to generate equivalent atoms: For **1**: #1 $-x+1, y+1/2, -z+1/2$; #2 $x, -y+1/2, z-1/2$. For **2**, **6** and **9**: #1 $-x+1/2, -y+1/2, -z$. For **3**: #1 $-x+y-2/3, -x+2/3, z-1/3$. For **4**: #1 $-x, -y+1, -z+1$; #2 $-x+1, -y+1, -z+1$; #3 $x-1, y, z$; #4 $-x+2, -y, -z+1$; #5 $-x+1, -y+1, -z$; #6 $x+1, y-1, z+1$. For **7**: #1 $-x+1, -y, -z$. For **8**: #1 $-x+1, -y+1, -z$.

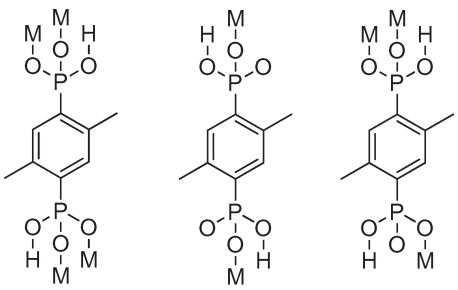

Scheme 1 Schematic presentation of the coordination modes of the diphosphonate ligands in compounds **1**–**9**.

together to form a three-dimensional structure *via* the linking of pyrazine molecules at the vertex positions of the NiO_4N_2 octahedrons (see Fig. 4b).

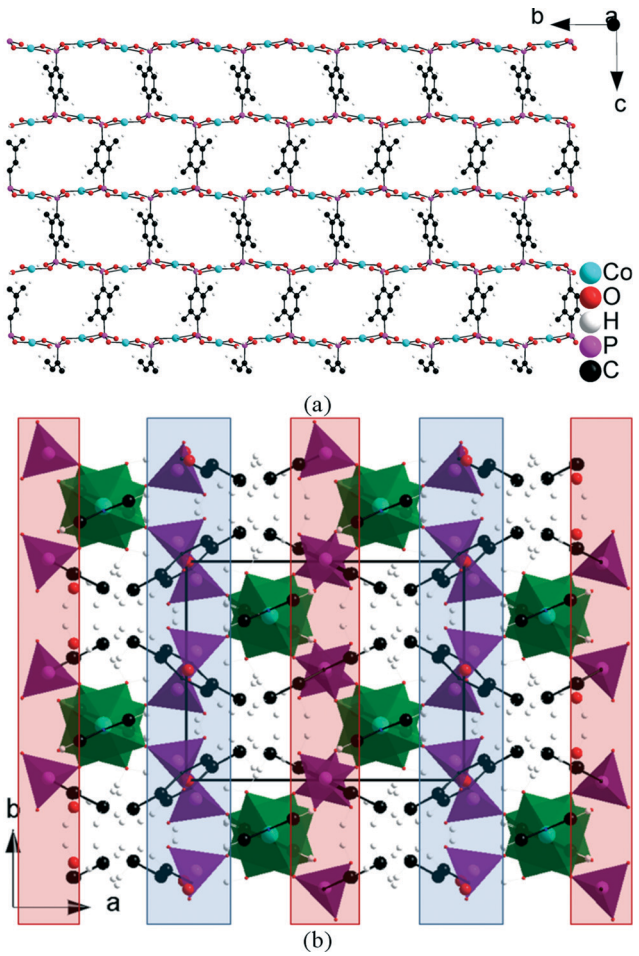

Fig. 2 Two-dimensional layer in the *bc*-plane constructed from Co(II) ions and model-A diphosphonate ligands (a) and three-dimensional packing diagram (b) of compound **1**. In (b) the two kinds of diphosphonate ligands are shaded in pink (model-A) and blue (model-B), respectively.

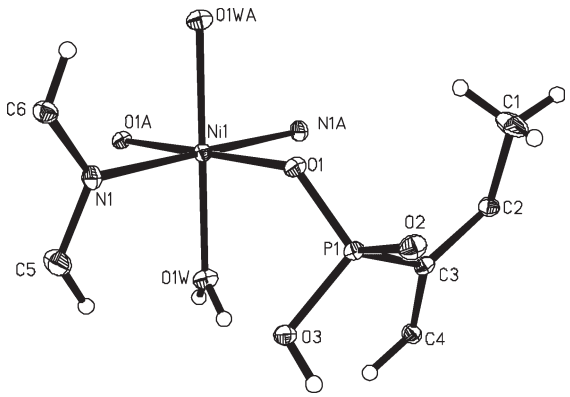

Fig. 3 Coordination environment of compound **2** (thermal ellipsoids are given at 30% probability). A: $0.5-x, 0.5-y, -z$.

Structure description of compound 3

Upon changing the second ligand from pyrazine to 2,2′-bipy, one new compound (**3**) with a new structure was obtained. The single-crystal X-ray diffraction analysis reveals that it has

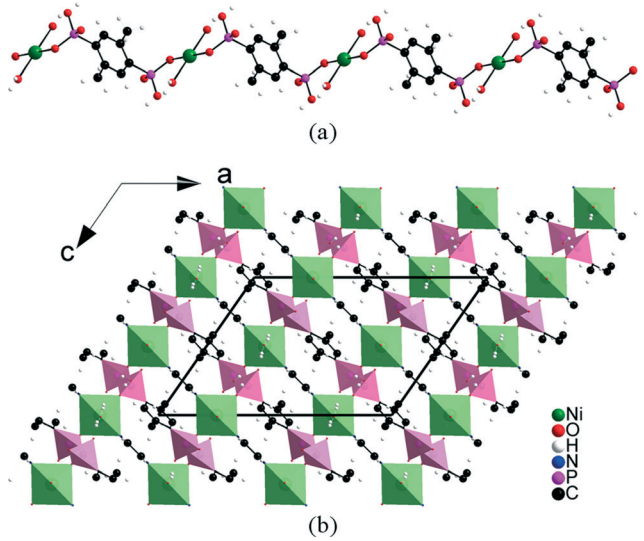

Fig. 4 One-dimensional chain (a) and three-dimensional packing diagram viewing along the *b*-direction (b) of compound **2**.

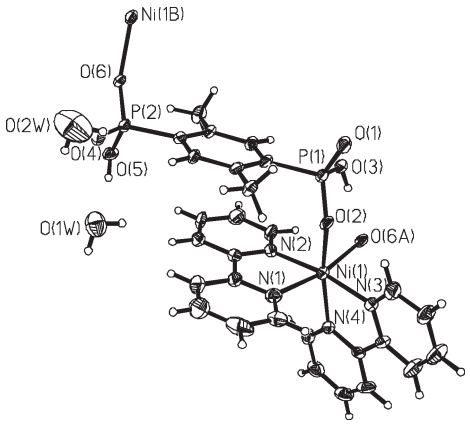

Fig. 5 XPREP diagram of compound **3** (thermal ellipsoids are given at 30% probability). A: 1 − *x*, −*y*, −*z*.

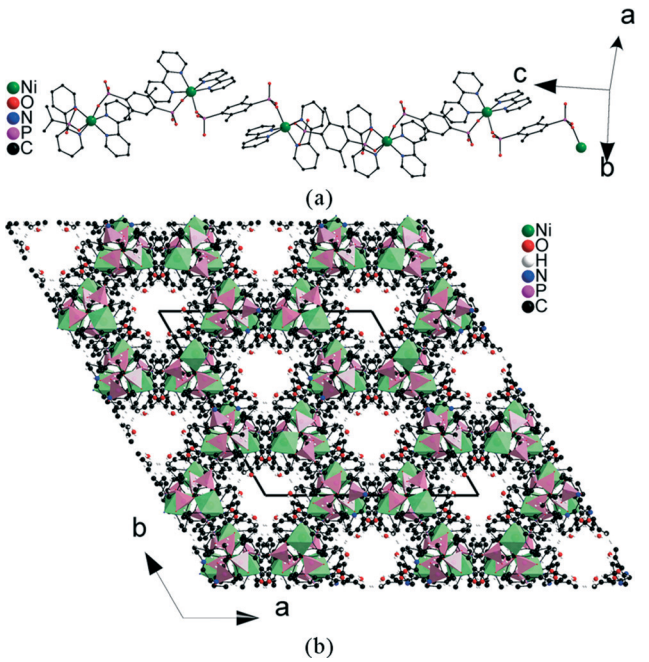

Fig. 6 One-dimensional helix chain along the *c*-direction (a) and three-dimensional packing diagram (b) of compound **3**.

a one-dimensional chain structure. It crystallizes in the trigonal space group *R*3*c* with eighteen molecules in each unit cell. Each asymmetric unit is comprised of one crystallographically independent Ni(II), one doubly deprotonated diphosphonate ligand, two 2,2′-bipy molecules and two lattice water molecules (Fig. 5), indicating a formula of $[Ni(H_2L)(2,2'\text{-bipy})_2][(H_2O)_2]$. The Ni(II) ion is octahedrally coordinated by four nitrogen atoms of two chelating 2,2′-bipy molecules and two phosphonate oxygen atoms from two diphosphonate ligands, with Ni–O and Ni–N bond lengths in the ranges of 2.059(11)–2.069(8) and 2.082(11)–2.118(8) Å (see Table 2), respectively, which are all in normal ranges.[14] In this case, the diphosphonate ligand is also doubly deprotonated and adopts the same coordination mode as that found in compounds **2**, **6** and **9** (mode-B in Scheme 1). These diphosphonate ligands behave as bidentate linkers and link the Ni(II) ions into an infinite one-dimensional helix chain along the *c*-axis (see Fig. 6a). A short center to center distance of 3.6505(1) Å is found for neighboring benzene and pyridine rings, indicating significant π···π interactions (dihedral angle: 9.11(3)°) between the diphosphonate ligands and 2,2′-bipy molecules. These 1D chains further assemble into a three-dimensional supramolecular structure forming hexagonal 1D channels running along the *c*-axis with diameters of about 4.818 Å (see Fig. 6b). The calculated void space is around 1554.3 $Å^3$, which amounts to 11.3% of the unit cell volume.

Structure description of compound 4

The 2,2′-bipy was further changed to 4,4′-bipy and this resulted in a new compound. Single-crystal X-ray diffraction analysis reveals that compound **4** crystallizes in the triclinic space group $P\bar{1}$ and displays a three-dimensional pillar-layered structure. The asymmetric unit consists of two crystallographically independent Ni(II) ions lying at special positions (0, 0.5, 0.5 and 1.0, 0, 0.5), one 4,4′-bipy, one coordinating and two lattice water molecules (see Fig. 7). Both Ni1 and Ni2 are six-coordinated, but the first coordination sphere of Ni1 is filled by two nitrogen atoms of two 4,4′-bipy molecules and four phosphonate oxygen atoms of four diphosphonate ligands, whereas Ni2 is coordinated by two aqua ligands, two nitrogen atoms and two phosphonate oxygen atoms. The coordination mode of the diphosphonate is different from those of the above mentioned compounds. In this case, one phosphonate group is monodentate whereas another one is bidentate. Its coordination mode can be denoted as: $\mu^3{:}\eta^0{:}\eta^0{:}\eta^1{:}\eta^0{:}\eta^1{:}\eta^1$ (model-C, see Scheme 1). These bridging ligands link the Ni(II) ions into a two-dimensional layer structure in the

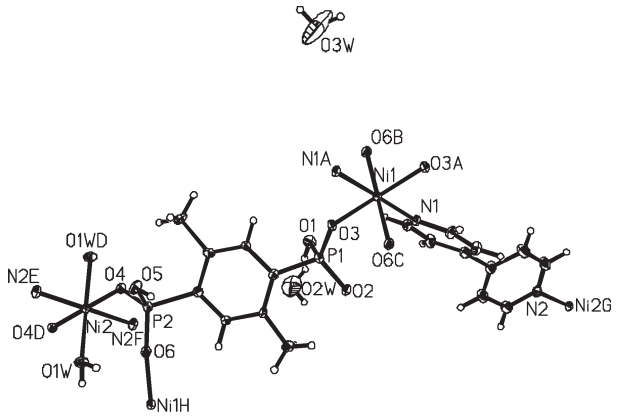

Fig. 7 XPREP diagram of compound **4** with 50% probability. A: −*x*, 1 − *y*, 1 − *z*; B: −1 + *x*, *y*, *z*; C: 1 − *x*, 1 − *y*, 1 − *z*; D: 2 − *x*, −*y*, 1 − *z*; E: 1 + *x*, −1 + *y*, 1 + *z*; F: 1 − *x*, 1 − *y*, −*z*; G: −1 + *x*, 1 + *y*, −1 + *z*; H: 1 + *x*, *y*, *z*.

ab-plane (see Fig. 8a). The bridging linkers 4,4′-bipy bind at the apical positions of the Ni1 octahedrons and form a three-dimensional pillar layered structure with a distance of about 10.7556 Å between neighboring layers (see Fig. 8b). The lattice water molecules are accommodated between the layers and form plenty of O–H···O interactions with the aqua ligands and uncoordinated phosphonate oxygen atoms (see Table S1†).

Structure description of compound 5

The auxiliary N-donor ligand was further changed to a longer one (dpe) to investigate its effect on the structure formation. As expected, the structure of the obtained compound is very different to those of compounds 2–4. It crystallizes in the triclinic $P\bar{1}$ space group. In the asymmetric unit, there is one crystallographically independent Ni(II) ion, two diphosphonate and dpe ligand segments lying at inversion centers, two aqua ligands and two lattice water molecules (see Fig. 9). Each Ni(II) ion is six-coordinated by two phosphonate oxygen atoms of two diphosphonate ligands, two nitrogen atoms of two dpe molecules and two water oxygen atoms, forming an octahedron with the Ni–O and Ni–N bond lengths in the ranges of 2.045(3)–2.102(3) and 2.107(3)–2.118(3) Å (see Table 2), respectively, which are comparable to those of other reported nickel(II) phosphonates.[14] The diphosphonate ligands also adopt a model-B coordination mode and behave as linkers which bridge the Ni(II) ions into a one-dimensional infinite chain along the (221)-direction (see Fig. 10a). These 1D chains are further connected by the dpe ligands into a square grid in the *ac*-plane (see Fig. 10b). A closer look at the structure of the layers reveals that all the coordinating water molecules point at interlayers, whereas the uncoordinating water molecules exist around the aqua ligands between layers. These water molecules are involved in the formation of H-bonding interactions with the uncoordinated phosphonate oxygen atoms, behaving as hydrogen donors or acceptors (see Table S1†). Thus, these square grids are assembled into

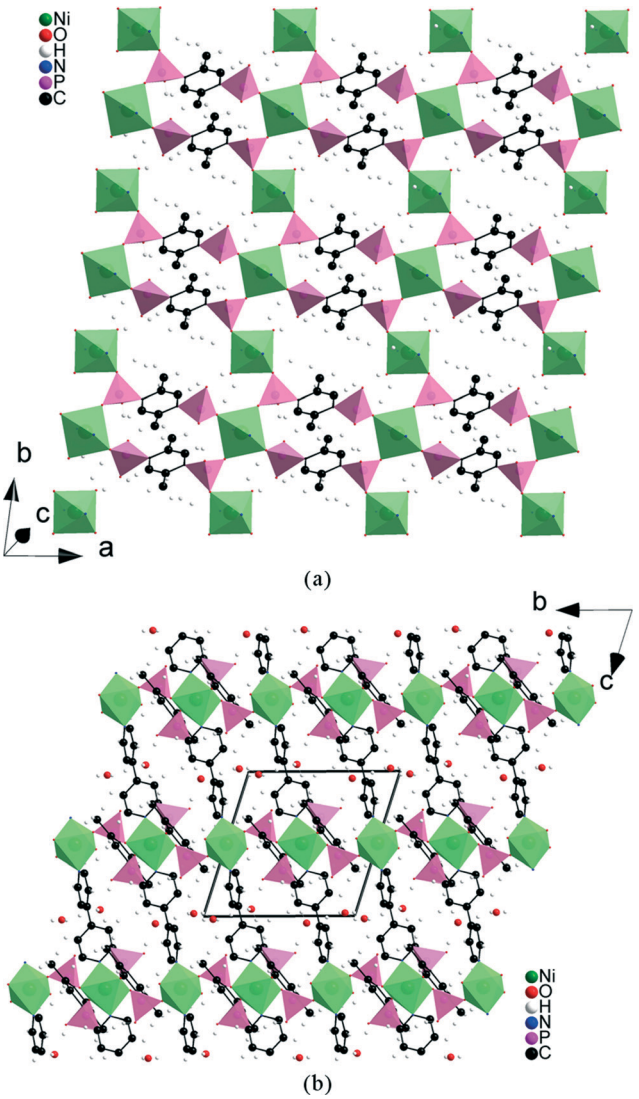

Fig. 8 Two-dimensional layer (a) and three-dimensional packing diagram (b) of compound **4**.

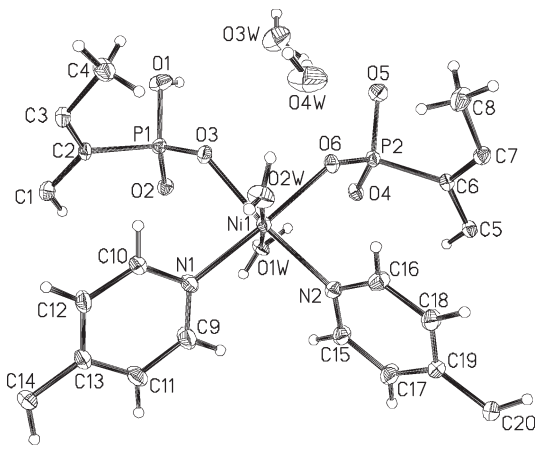

Fig. 9 XPREP diagram of compound **5** (thermal ellipsoids are given at 30% probability).

a three-dimensional supramolecular structure with the aid of these H-bonds (see Fig. 10c).

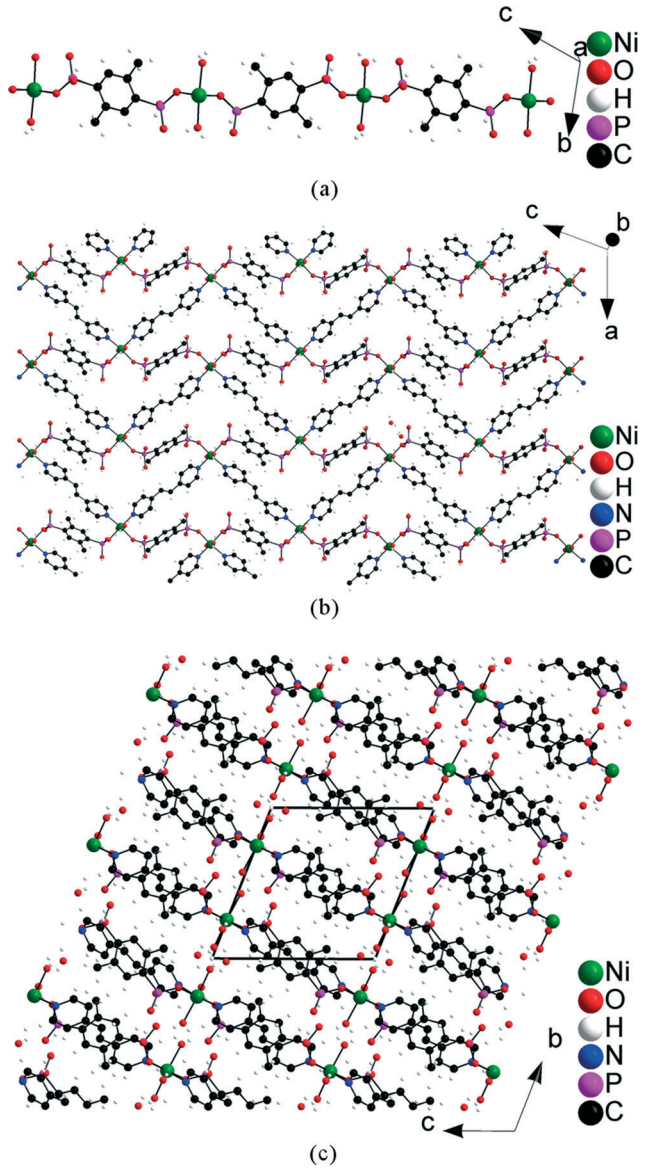

Fig. 10 One-dimensional chain along the (221)-direction (a), two-dimensional layer in the *ac*-plane (b) and three-dimensional packing diagram viewing along the *a*-direction (c) of compound **5**.

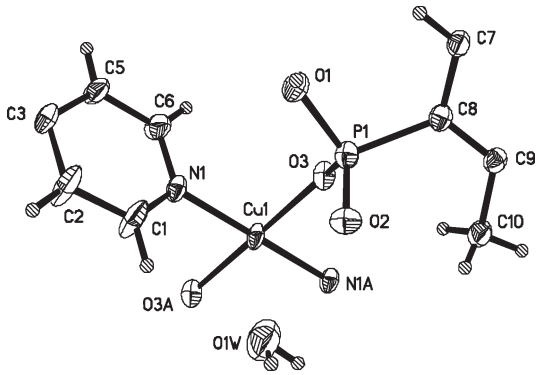

Fig. 11 XPREP diagram of compound **7** (thermal ellipsoids are given at 30% probability). A: 1 − *x*, −*y*, −*z*.

Structure description of compound 7

The diphosphonate ligand was also reacted with $CuSO_4{\cdot}5H_2O$ and 4,4′-bipy, leading to the formation of compound **7**. It is very interesting that the structure of this compound is very different to that of **5**, but very similar to that of **4**, which has a layered structure. The asymmetric unit consists of one crystallographically independent Cu(II) ion lying at a special position (0.5, 0, 0), a half diphosphonate ligand and 4,4′-bipy molecule lying at inversion centers, and one water molecule (see Fig. 11), corresponding to a formula of $[Cu(H_2L)(4,4'\text{-bipy})][(H_2O)_2]$. The Cu(II) ion is square-planar coordinated by two symmetry related phosphonate oxygen atoms of two diphosphonate ligands and two symmetry related nitrogen atoms of two 4,4′-bipy molecules (see Fig. 11), with the Cu–O and Cu–N bond lengths found to be 1.935(3) and 1.998(3) Å, respectively (see Table 2), which are comparable to those of other reported copper(II) phosphonates.[15] A model-B coordination mode is also observed for the diphosphonate ligand. These bidentate ligands bridge the Cu(II) ions into one-dimensional infinite chains along the (022)-direction (see Fig. 12a), which are further assembled by 4,4′-bipy molecules into two-dimensional square-grid sheets in the *ac*-plane (see Fig. 12b). It should be noted there are two symmetry-related water molecules above and below the square planar coordination geometry of the Cu(II) ion which form weak bonding with the Cu(II) center (Cu–O1W: 2.890(5) Å) and very weak interactions with the phosphonate groups, leading to the formation of one three-dimensional supramolecular structure (see Fig. 12c).

Structure description of compound 8

Compound **8** crystallizes in the triclinic $P\bar{1}$ space group with two molecules in each unit cell. The asymmetric unit consists of one Zn(II) ion, two diphosphonate ligand segments lying at inversion centers and one 2,2′-bipy molecule (see Fig. 13), suggesting a formula of $[Zn(H_2L)(2,2'\text{-bipy})]$. The coordination geometry around the Zn(II) center can be regarded as a distorted trigonal bipyramid with O3 and N1 lying at the axial positions and O1, O6 and N2 at the equatorial positions. The Zn–O and Zn–N bond lengths are found to be in the ranges of 1.955(2)–2.038(2) and 2.119(3)–2.174(3) Å (see Table 2), respectively, which are all comparable to those of other Zn-containing compounds.[16] The two crystallographically independent diphosphonate ligands adopt two kinds of coordination modes: A and B (see Scheme 1). With the linkage of these ligands, the Zn(II) ions are woven into square grids in the *ab*-plane (see Fig. 14a). The uncoordinated phosphonate oxygen atoms are involved in the formation of O···O interactions (see Table S1†) and give rise to a three-dimensional supramolecular structure (see Fig. 14b).

Effect of the auxiliary ligands on the structure formation

In this work, a series of pyridine-containing auxiliary ligands with different sizes and shapes were employed as second

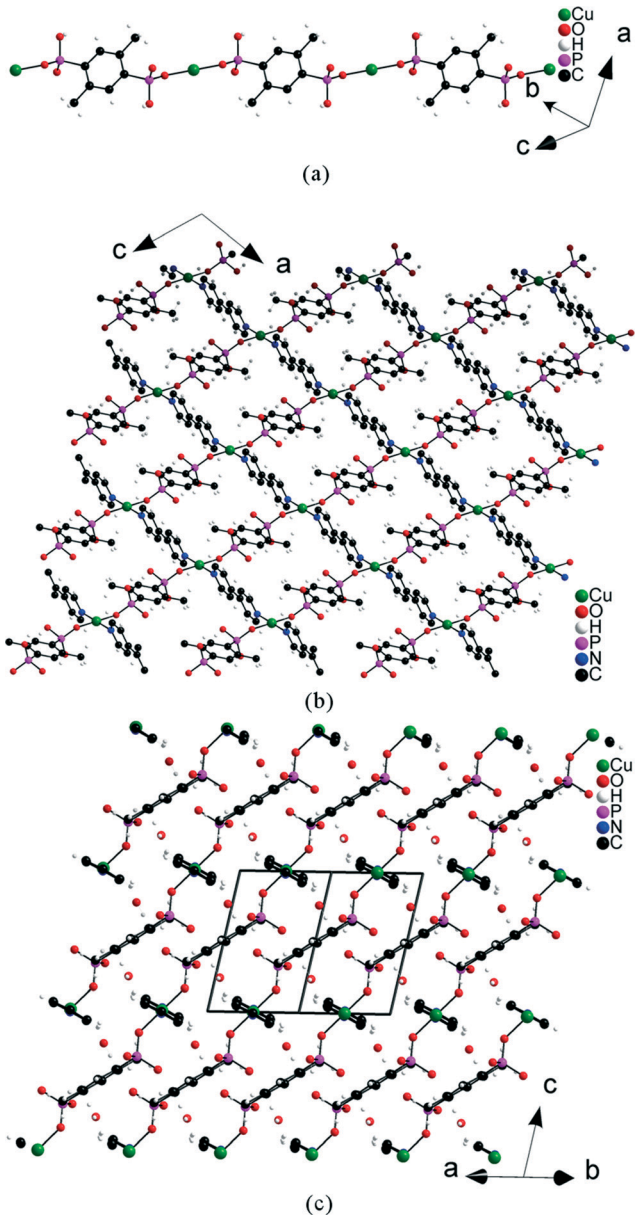

Fig. 12 One-dimensional chain along the (022)-direction (a), two-dimensional layer in the *ac*-plane (b) and three-dimensional packing diagram viewing along the (220)-direction (c) of compound **7**.

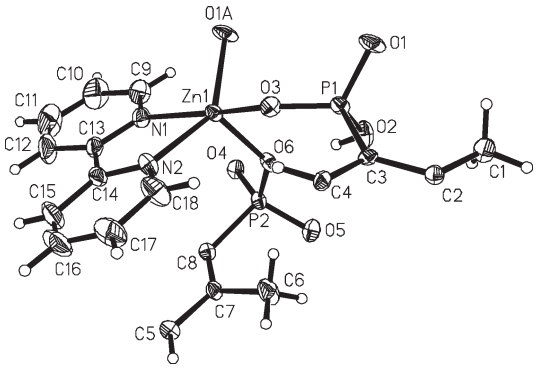

Fig. 13 XPREP diagram of compound **8** (thermal ellipsoids are given at 30% probability). A: $-x + 1, -y + 1, -z$.

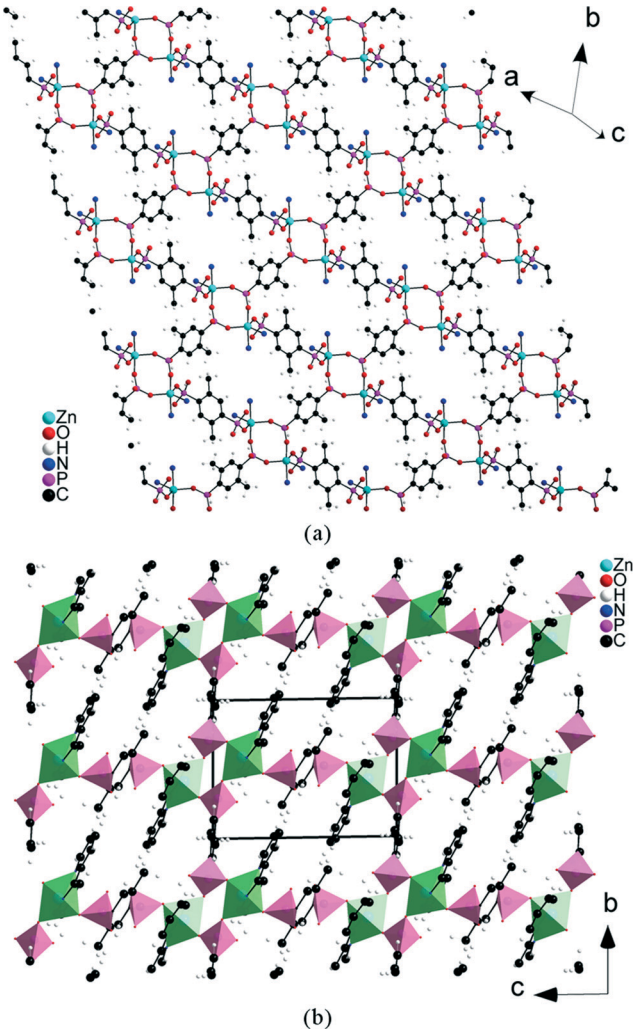

Fig. 14 Two-dimensional layer structure viewing along the (1 −2 1) direction (a) and three-dimensional supramolecular packing structure viewing along the *a*-axis (b) of compound **8**.

ligands to investigate their effect on the structure formation. From the structural analysis results it is obvious that low dimensionality is expected when 2,2′-bipy is used, whereas linear linkers such as pyrazine, 4,4′-bipy and dpe, not always but most of time, prefer to form three-dimensional framework structures. Among the four linear auxiliary ligands, undoubtedly pyrazine is the shortest one (2.797 Å). Four of the nine compounds (**1**, **2**, **6** and **9**) contain pyrazine ligands and display three-dimensional framework structures. 4,4′-Bipy and dpe are much longer (4,4′-bipy: 7.107 Å, dpe: 9.393 Å); the former can be found in compounds **4** and **7** and the latter can be found in compound **5**. In these three compounds, **5** and **7** have square grid 2D layered structures, whereas **4** displays a three-dimensional pillar-layer structure. A closer look at their structures reveals that the M(II)···M(II) distances across the pyrazine linkers are 7.326 Å in **1**, 7.163 Å in **2**, 7.015 Å in **6** and 7.428 Å in **9**; all are comparable to the distance of the diphosphonate H_2L^{2-} ligand (~7.386 Å). The M(II)···M(II) distances across 4,4′-bipy or dpe are found to be 11.284,

13.620 and 11.034 Å for **4**, **5** and **7**, respectively, obviously longer than the length of the H_2L^{2-} ligand. Thus, it is clear the distance of the auxiliary ligand has a major effect on the structure formation and we would propose that a high dimensional structure is favoured when the M(II)···M(II) distance across the auxiliary ligand matches the distance of the diphosphonate linker.

PXRD and thermogravimetric analyses

Powder X-ray diffraction measurements (PXRD) for complexes **1–9** were performed to characterize their purity (Fig. S2–S10, ESI†). All the diffraction peaks on the curves are in good agreement with the simulated ones.

Thermogravimetric analyses were performed to investigate the thermal stability of compounds **1–9** (see Fig. 15). The TGA curve of compound **1** indicates that it is stable up to 160 °C. An initial weight loss (9.04%) of the lattice and coordinated water molecules is observed in the temperature range of 160–250 °C. The observed value is obviously larger than the calculated value (5.49%), indicating that more lattice water molecules are accommodated in the framework. After the removal of water molecules, a second weight loss, corresponding to the removal of pyrazine molecules (calculated: 18.78%, observed: 18.72%), starts immediately. The TGA curves of compounds **2**, **6** and **9** display similar character which is expected for isostructural compounds. Compounds **2** and **6** start to lose weight from 70 °C whereas compound **9** starts at about 150 °C, indicating better stability of **9**. For compound **3**, the first weight loss (5.79%) is observed in the range of 25–160 °C, corresponding to the removal of two coordinated water molecules in each formula (calculated: 5.37%). Following the first weight loss is a plateau until 300 °C. From the single-crystal X-ray diffraction analysis, compound **3** has a 1D chain structure, and normally moderate stability is expected. But the decomposition of **3** starts at about 300 °C, indicating its good thermal stability and strong π···π interactions between the 2,2′-bipy molecules. Several steps of weight losses are present on the TGA curve of compound **4**. The first one (12.11%), in the range of 30–130 °C, corresponds to the removal of two lattice and one coordinated water molecules (10.14%). It starts to decompose at about 195 °C, accompanying the release of 4,4′-bipy molecules. The thermal stability of compound **5** is not good; it starts to lose weight at about 60 °C and releases all the lattice and coordinated water molecules at about 245 °C. Upon further heating, the collapse of the coordination network is observed, accompanying the release of dpe ligands. The thermal stability of compound **7** is much better. No obvious weight loss can be observed before 155 °C. The first weight loss (7.16%) in the range of 155–220 °C, matches well with the value of two coordinated water molecules in each formula (6.93%). It does not decompose until the temperature reaches 300 °C, whereafter it begins to decompose. For compound **8**, it starts to decompose at about 320 °C, indicating very good thermal stability which can be ascribed to the contribution of the strong π···π interaction between the pyridine and benzene rings and O···O bonds in the 3D supramolecular structure.

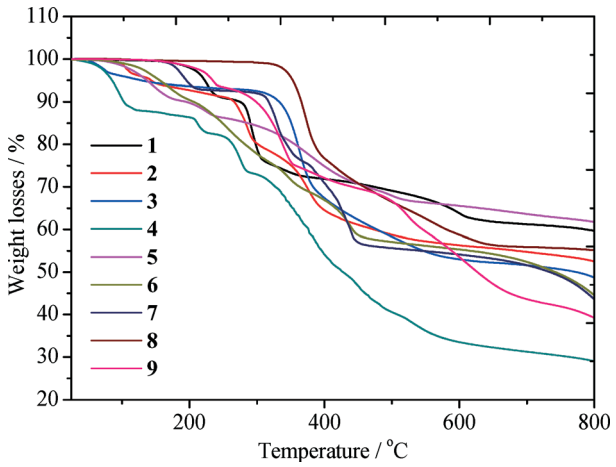

Fig. 15 TGA diagrams of compounds **1–9**.

Photoluminescence properties

Zn(II) and Cd(II)-containing compounds have received much attention for their potential applications as optical materials or chemical sensors. Thus, the photoluminescence properties of compounds **8** and **9**, as well as the free diphosphonate ligand, 2,2′-bipy and pyrazine, were investigated in the solid state at room temperature (see Fig. 16). It was found the free ligands display photoluminescence with emission maxima at about 318 nm for H_4L, 359 and 397 (shoulder) nm for pyz, and 544 nm for 2,2-bipy, respectively. It can be presumed that these emissions originated from the π* → π or π* → n transitions. Upon complexation with Zn(II) and Cd(II) ions, intense fluorescence emissions are observed at 369 and 387 (shoulder) nm for **8**, and 415.5 nm for **9**. Comparing with the emissions of the free ligands, different band shapes and blue or red shifts have been observed for compounds **8** and **9**. Considering that Zn(II) and Cd(II) ions are difficult to oxidize or reduce,[17] these bands can also be ascribed to intraligand fluorescence emissions which are largely affected by the different coordination environments around the respective metal centers and different deprotonation levels of the H_4L ligands.[18]

Magnetic properties

The variable-temperature susceptibilities (χ_m) of compounds **1–3** were investigated on polycrystalline samples over the temperature range 2–300 K with a 1 kOe applied field (see Fig. 17–19).

For **1**, the observed $\chi_m T$ value at room temperature is 3.52 cm^3 K mol^{-1}, which is slightly lower than the spin-only value of 3.87 cm^3 K mol^{-1} expected for one isolated high spin Co^{II} ion with $S = 3/2$ and $g = 2.00$. As the temperature is lowered, the $\chi_m T$ value decreases gradually to reach a minimum of 0.51 cm^3 K mol^{-1} at 2 K, suggesting an overall antiferromagnetic interaction (see Fig. 17). The reciprocal molar

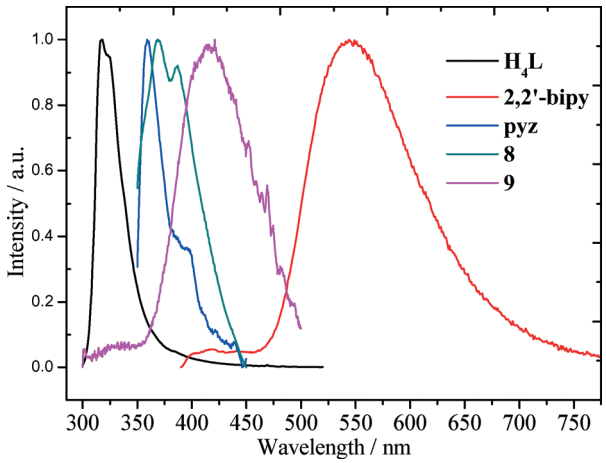

Fig. 16 Normalized emission spectra of H_4L, 2,2′-bipy, pyrazine, and compounds **8** and **9**.

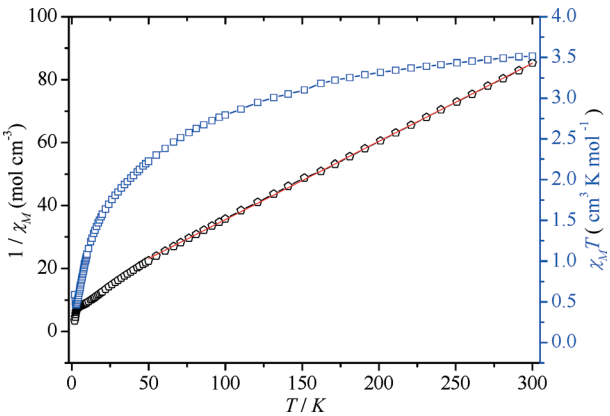

Fig. 17 Plots of the temperature dependence of $\chi_M T$ and χ_M^{-1} for compound **1**.

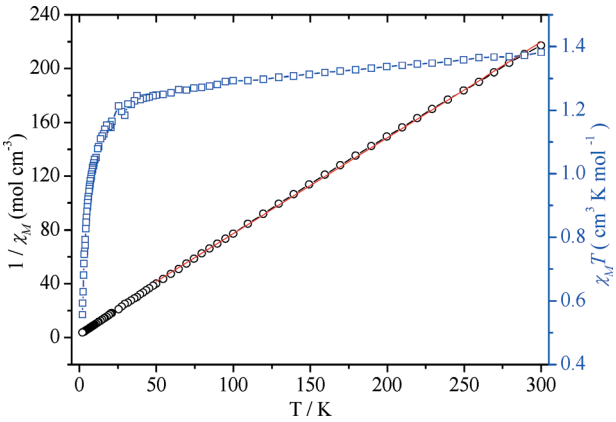

Fig. 18 Plots of the temperature dependence of $\chi_M T$ and χ_M^{-1} for compound **2**.

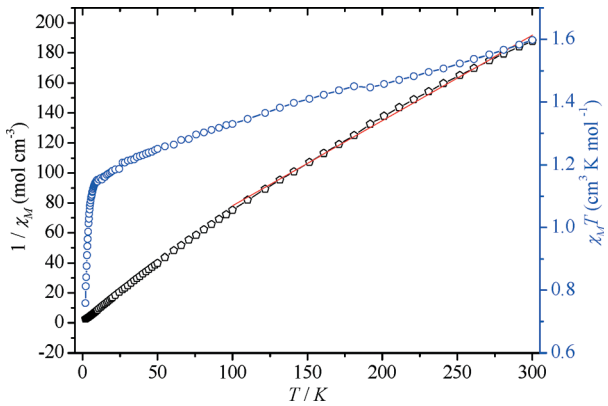

Fig. 19 Plots of the temperature dependence of $\chi_M T$ and χ_M^{-1} for compound **3**.

magnetic susceptibility data obey the Curie–Weiss law well in the high temperature region of 50–300 K, with a Curie constant of C = 4.0 cm^3 K mol^{-1} and a Weiss constant of θ = −42.64 K. The negative value of the Weiss temperature suggests an antiferromagnetic interaction.[19]

The magnetic properties of compounds **2** and **3** in the form χ_M^{-1} and $\chi_M T$ *vs.* T are represented in Fig. 18–19. Fitting of the susceptibility data according to the Curie–Weiss law gives Curie constants (C) of 1.40 and 1.76 cm^3 K mol^{-1} for **2** (50–300 K) and **3** (100–300 K), respectively, and Weiss constants (θ) of −8.62 and −37.21 K for **2** and **3**, respectively. At room temperature, the values of $\chi_M T$ are 1.38 and 1.60 cm^3 K mol^{-1} for **2** and **3**, respectively, which are slight higher than the expected value of 1.21 cm^3 K mol^{-1} for one spin-only Ni^{2+} (S = 1) ion with g = 2.2. This difference might be caused by the spin-orbit coupling characteristic for nickel(II) complexes with $^3A_{2g}$ ground states.[20] Upon cooling, the $\chi_M T$ value declines continuously and reaches values of 0.56 and 0.76 cm^3 K mol^{-1} at 2.0 K for **2** and **3**, respectively, suggesting a dominant antiferromagnetic exchange behavior between neighboring Ni^{2+} ions.

In compounds **1** and **2**, the M(II) ions are bridged by the pyrazine and bidentated diphosphonate ligands H_2L^{2-} with M(II)···M(II) distances of 7.326 and 9.962 Å for **1**, and 7.163 and 9.648 Å for **2**. The magnetic exchange coupling is, therefore, mainly propagated through the pyrazine bridges. For compound **3**, the Ni(II) centers are bridged through the long bridging ligands H_2L^{2-}. As the shortest Ni(II)···Ni(II) distance across the diphosphonate ligands is 10.077 Å, the magnetic exchange coupling through the H_2L^{2-} bridge is expected to be very weak. The overall antiferromagnetic interaction should be mainly attributed to the superexchange coupling between the 1D chains. It is noticed that the shortest Co···Co distance between the 1D chains in **3** is 8.334 Å.[21]

Conclusion

In summary, a series of metal diphosphonates with different second auxiliary ligands and structures have been synthesized and thoroughly characterized. The crystal structural analyses reveal that the size of the second auxiliary ligand has a large effect on the structure formation. High-dimensional structure is favoured when the M(II)···M(II) distance across the auxiliary ligand matches the distance of the diphosphonate linker. The Zn- and Cd-containing

compounds (**8** and **9**) display interesting intraligand fluorescent emissions. The Co- and Ni-containing compounds (**1**–**3**) all show dominant antiferromagnetic exchange behaviors.

Acknowledgements

This work was supported by the National Natural Science Foundation of China (no. 21171173 and 21173246).

Notes and references

1 (*a*) K. J. Gagnon, H. P. Perry and A. Clearfield, *Chem. Rev.*, 2012, **112**, 1034–1054; (*b*) *Metal phosphonate chemistry: From synthesis to application*, ed. A. Clearfield and K. D. Demadis, The Royal Society of Chemistry, London, 2012.

2 (*a*) S. R. Miller, G. M. Pearce, P. A. Wright, F. Bonino, S. Chavan, S. Bordiga, I. Margiolaki, N. Guillou, G. Férey, S. Bourrelly and P. L. Llewellyn, *J. Am. Chem. Soc.*, 2008, **130**, 15967–15981; (*b*) M. Taddei, F. Costantino, A. Ienco, A. Comotti, P. V. Daud and S. M. Cohen, *Chem. Commun.*, 2013, **49**, 1315–1317.

3 (*a*) M. Angeloni, O. Piermatti, F. Pizzo and L. Vaccaro, *Eur. J. Org. Chem.*, 2014, 1716–1726; (*b*) Y.-P. Zhu, Y.-L. Liu, T.-Z. Ren and Z.-Y. Yuan, *RSC Adv.*, 2014, **4**, 16018–16021; (*c*) A. Dutta, A. K. Patra, H. Uyama and A. Bhaumik, *ACS Appl. Mater. Interfaces*, 2013, **5**, 9913–9917.

4 (*a*) C. Maxim, D. G. Branzea, C. Tiseanu, M. Rouzières and R. Clérac, *Inorg. Chem.*, 2014, **53**, 2708–2717; (*b*) R. M. P. Colodrero, K. E. Papathanasiou, N. Stavgianoudaki, P. Olivera-Pastor, E. R. Losilla, M. A. G. Aranda, L. León-Reina, J. Sanz, I. Sobrados, D. Choquesillo-Lazarte, J. M. García-Ruiz, P. Atienzar, F. Rey, K. D. Demadis and A. Cabeza, *Chem. Mater.*, 2012, **24**, 3780–3792; (*c*) R. Janicki, M. Monteil, M. Lecouvey and A. Mondry, *Opt. Mater.*, 2013, **36**, 259–264.

5 X. Yang, S.-S. Bao, M. Ren, N. Hoshino, T. Akutagawa and L.-M. Zheng, *Chem. Commun.*, 2014, **50**, 3979–3981.

6 (*a*) Z. Chen, Y. Ling, H. Yang, Y. Guo, L. Weng and Y. Zhou, *CrystEngComm*, 2011, **13**, 3378–3382; (*b*) S. Comby, R. Scopelliti, D. Imbert, L. Charbonnière, R. Ziessel and J.-C. G. Bünzli, *Inorg. Chem.*, 2006, **45**, 3158–3160; (*c*) P. F. Wang, D. K. Cao, S. S. Bao, H. J. Jin, Y. Z. Li, T. W. Wang and L. M. Zheng, *Dalton Trans.*, 2011, **40**, 1307–1312; (*d*) D. K. Cao, M. J. Liu, J. Huang, S. S. Bao and L. M. Zheng, *Inorg. Chem.*, 2011, **50**, 2278–2287; (*e*) H. E. Moll, A. Dolbecq, I. M. Mbomekalle, J. Marrot, P. Deniard, R. Dessapt and P. Mialane, *Inorg. Chem.*, 2012, **51**, 2291–2302; (*f*) Z.-Y. Du, H.-B. Xu and J.-G. Mao, *Inorg. Chem.*, 2006, **45**, 6424–6430; (*g*) X.-L. Zhang, K. Cheng, F. Wang and J. Zhang, *Dalton Trans.*, 2014, **43**, 285–289.

7 (*a*) W. Yang, H. Y. Wu, R. X. Wang, Q. J. Pan, Z. M. Sun and H. Zhang, *Inorg. Chem.*, 2012, **51**, 11458–11465; (*b*) L. Zhang, B. Marzec, R. Clérac, Y. Chen, H. Zhang and W. Schmitt, *Chem. Commun.*, 2013, **49**, 66–68; (*c*) Y. S. Ma, Y. Z. Li, Y. Song and L. M. Zheng, *Inorg. Chem.*, 2008, **47**, 4536–4544; (*d*) P. Ramaswamy, R. Prabhu and S. Natarajan, *Inorg. Chem.*, 2010, **49**, 7927–7934.

8 S. F. Tang, L. J. Li, X. X. Lv, C. Wang and X. B. Zhao, *CrystEngComm*, 2014, **16**, 7043–7052.

9 *SAINT, Version 6.45*, Bruker Analytical X-ray Systems Inc., 2003.

10 G. M. Sheldrick, *SADABS, Version 2.10*, Bruker AXS Inc., Madison, WI, 2003.

11 G. M. Sheldrick, *SHELXS-97, Program for Crystal Structure Solution and Refinement*, University of Göttingen, 1997.

12 G. M. Sheldrick, *SHELXTL, Crystallographic Software Package, SHELXTL, Version 5.1*, Bruker-AXS, Madison, WI, 1998.

13 (*a*) S.-P. Shi, Y.-Y. Zhu, Z.-G. Sun, W. Zhou, L.-L. Dai, M.-X. Ma, W.-Z. Li, H. Luo and T. Sun, *Cryst. Growth Des.*, 2014, **14**, 1580–1590; (*b*) T. Zheng, S.-S. Bao, M. Ren and L.-M. Zheng, *Dalton Trans.*, 2013, **42**, 16396–16402.

14 (*a*) B. K. Tripuramallu, R. Kishore and S. K. Das, *Polyhedron*, 2010, **29**, 2985–2990; (*b*) S.-F. Tang, X.-B. Pan, X.-X. Lv and X.-B. Zhao, *J. Solid State Chem.*, 2013, **197**, 139–146.

15 (*a*) V. Georgantas, M. Menelaou, V. Psycharis, C. P. Raptopoulou, A. Terzis, V. Tangoulis, C. Mateescu and A. Salifoglou, *Inorg. Chem.*, 2013, **52**, 4963–4976; (*b*) J. Huang, P.-Y. Liu, H. Zhu, S.-S. Bao, L.-M. Zheng and J. Ma, *ChemPlusChem*, 2012, **77**, 1087–1095.

16 (*a*) R. Fu, S. Hu and X. Wu, *CrystEngComm*, 2013, **15**, 8937–8940; (*b*) K. J. Gagnon, A. V. Prosvirin, K. R. Dunbar, S. J. Teat and A. Clearfield, *Dalton Trans.*, 2012, **41**, 3995–4006; (*c*) L.-M. Li, K. Cheng, F. Wang and J. Zhang, *Inorg. Chem.*, 2013, **52**, 5654–5656.

17 (*a*) X. He, X.-P. Lu, M.-X. Li and R. E. Morris, *Cryst. Growth Des.*, 2013, **13**, 1649–1654; (*b*) D. Sun, L.-L. Han, S. Yuan, Y.-K. Deng, M.-Z. Xu and D.-F. Sun, *Cryst. Growth Des.*, 2013, **13**, 377–385; (*c*) L. Wen, Z. Lu, J. Lin, Z. Tian, H. Zhu and Q. Meng, *Cryst. Growth Des.*, 2007, **7**, 93–99.

18 J.-X. Yang, X. Zhang, J.-K. Cheng, J. Zhang and Y.-G. Yao, *Cryst. Growth Des.*, 2012, **12**, 333–345.

19 J.-S. Hu, X.-Q. Yao, M.-D. Zhang, L. Qin, Y.-Z. Li, Z.-J. Guo, H.-G. Zheng and Z.-L. Xue, *Cryst. Growth Des.*, 2012, **12**, 3426–3435.

20 (*a*) A. Earnshaw, *Introduction to Magnetochemistry*, Academic Press, London, 1968; (*b*) R. L. Carlin, *Magnetochemistry*, Springer, Berlin, 1986.

21 (*a*) J.-G. Lin, Y. Su, Z.-F. Tian, L. Qiu, L.-L. Wen, Z.-D. Lu, Y.-Z. Li and Q.-J. Meng, *Cryst. Growth Des.*, 2007, **7**, 2526–2534; (*b*) L. M. Zheng, X. Q. Wang, Y. S. Wang and A. J. Jacobson, *J. Mater. Chem.*, 2001, **11**, 1100.